



## Optimal Fractal-Like Hierarchical Honeycombs

Ramin Oftadeh,<sup>1</sup> Babak Haghpanah,<sup>1</sup> Dominic Vella,<sup>2</sup> Arezki Boudaoud,<sup>3</sup> and Ashkan Vaziri<sup>1,\*</sup>

<sup>1</sup>Department of Mechanical and Industrial Engineering, Northeastern University, Boston, Massachusetts 02115, USA

<sup>2</sup>Mathematical Institute, University of Oxford, Woodstock Road, Oxford OX2 6GG, United Kingdom

<sup>3</sup>Laboratoire Reproduction et Développement des Plantes and Laboratoire Joliot-Curie, INRA, CNRS, ENS, Université de Lyon, 46 Allée d'Italie, F-69364 Lyon Cedex 07, France

(Received 3 June 2014; published 3 September 2014)

Hexagonal honeycomb structures are known for their high strength and low weight. We construct a new class of fractal-appearing cellular metamaterials by replacing each three-edge vertex of a base hexagonal network with a smaller hexagon and iterating this process. The mechanical properties of the structure after different orders of the iteration are optimized. We find that the optimal structure (with highest in-plane stiffness for a given weight ratio) is self-similar but requires higher order hierarchy as the density vanishes. These results offer insights into how incorporating hierarchy in the material structure can create low-density metamaterials with desired properties and function.

DOI: 10.1103/PhysRevLett.113.104301

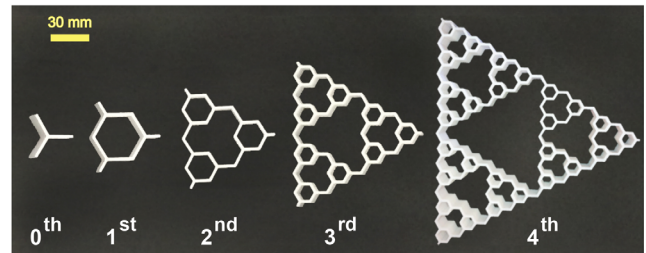
PACS numbers: 46.35.+z, 45.10.-b, 46.70.De

Hierarchically structured material systems are characterized by the existence of structure at different length scales and often exhibit superior mechanical properties such as enhanced stiffness [1,2], strength [2,3], toughness [4–6], and negative Poisson's ratio [7–9]. They are used in many fields including polymers [10], composite structures [11–13], sandwich panel cores [14,15], and biomimetic systems [2,6,16]. Perhaps the simplest example of an object whose stiffness is increased by structure is the simple hexagonal honeycomb [17]: such objects are well known to have relatively high stiffness for their low density. Recent work has sought to improve the properties of such structures by hollowing out the elements and replacing them with repeating units [18]. Along these lines, we consider a new family of honeycomb structures with a hierarchical refinement scheme in which the structural hexagonal lattice is replaced by smaller hexagons. This process can be repeated to create honeycombs of higher hierarchical order (see Fig. 1). As well as being a natural way to generate hierarchy, a similar structure has previously been proposed as a natural one for a two-dimensional soap froth to take [19–21] and is reminiscent of micrographs of polymeric foam which suggest two levels of hierarchy [2]. Such cellular solids have previously been shown to have improved in-plane stiffness and strength compared to the corresponding regular honeycombs [1,22,23]. However, it is still unknown whether such structures can be systematically optimized, in particular by adjusting the number of hierarchies that are used. In this Letter, the optimal configuration of such hierarchical honeycombs in the sense of highest elastic modulus is determined for various structural densities using finite element simulation, scaling analysis, and experiments.

The structural organization (a set of real numbers  $\gamma_i$ ) is defined by the ratio of the newly introduced hexagonal edge

length ( $l_i$ ) to previous hexagon edge length ( $l_{i-1}$ ) where  $i$  varies from 2 to  $n$  (hierarchical order) (i.e.,  $\gamma_i = l_i/l_{i-1}$ ). For convenience,  $\gamma_1$  is defined as  $2l_1/l_0$  (see below). Some geometric constraints on the hierarchically introduced edges must be imposed to avoid overlapping with preexisting

(a)



(b)

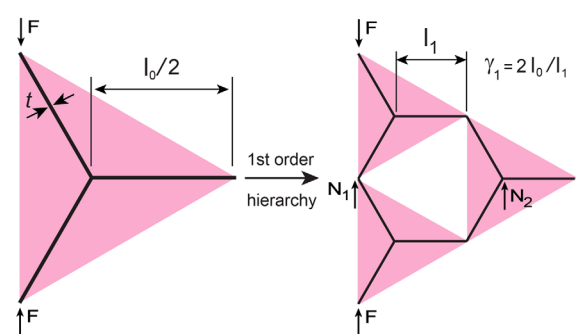


FIG. 1 (color online). (a) Unit cell of regular (i.e., zeroth) to fourth order hierarchical honeycombs fabricated using 3D printing. The physical thickness of the structures is constant,  $t_n = 2$  mm, because of the limitations of the 3D printing. To maintain the structure density, therefore, the size of this unit cell increases as the order of the hierarchy increases. (b) Unit cell of the hierarchical honeycombs with regular structure (left) and with first order hierarchy (right). Here  $F$  is an arbitrary concentrated force and  $N_1$  and  $N_2$  are the reaction forces at the midline.

edges. For the  $n$ th hierarchical order ( $n > 1$ ),  $0 \leq l_i \leq l_{i-1}$  and  $l_n \leq l_0 - \sum_{i=1}^{n-1} l_i$ , which can be written based on structural organization parameters as

$$\begin{aligned} 0 \leq \gamma_n \leq 1, \quad \text{and} \\ \sum_{i=1}^n \prod_{j=1}^i \gamma_j \leq 1, \end{aligned} \quad (1)$$

which must hold for all hierarchical orders ( $n \geq 1$ ). For simplicity, we assume that the wall thickness of  $t_n$  is uniform within a given structure; the relative density of the structure compared to the material density  $\rho_s$ , i.e.,  $\bar{\rho} = \rho/\rho_s$ , can be related to the length ratios  $\{\gamma_i\}$  and  $t_n/l_0$  via

$$\bar{\rho} = \frac{2}{\sqrt{3}} \left( 1 + \sum_{i=1}^n \prod_{j=1}^i \gamma_j \right) \frac{t_n}{l_0}. \quad (2)$$

This relation is used to adjust the thickness  $t_n$  to maintain a fixed relative density  $\bar{\rho}$  as the number of hierarchies, and the values of  $\gamma_i$ , are varied.

A hexagonal honeycomb network extending spatially to infinity has sixfold rotational symmetry. Classic symmetry arguments show that threefold symmetry is enough to guarantee an isotropic in-plane linear response for a two-dimensional solid [24]. The macroscopic in-plane elastic behavior of a hexagonal honeycomb structure is therefore isotropic and can be described by two elastic moduli, which we take to be the Young's modulus  $E$  and Poisson's ratio  $\nu$ . In this Letter, we focus on characterizing the effective Young's modulus of the structure  $E$ , measured relative to the Young's modulus of the basic honeycomb structure  $E_0$ . For numerical and analytical analysis, the far-field uniaxial stress in the vertical direction,  $\sigma_{yy} = (-2/3)F/l_0$ , was imposed to determine  $E$ . Here  $F$  is an arbitrary concentrated force; the vertical stress is equivalent to applying a force  $F$  in the vertical direction at the midpoint of every oblique edge in the original (i.e., zero hierarchy) hexagons (refer to the Supplemental Material for details [25]). To carry out the analysis, the unit cell of the lattice [Fig. 1(b)] was selected to represent the loaded lattice structure. Each beam in the lattice can undergo stretching, shear, and bending. In the bending dominated regime, the elastic modulus of the first order hierarchical honeycomb can be written as (see the Supplemental Material [25])

$$\frac{E_1}{E_0} = \frac{\sqrt{3}}{4} f(\gamma_1) \left( \frac{t_1}{t_0} \right)^3, \quad (3)$$

where  $E_0/E^m = (4/\sqrt{3})(t_0/l_0)^3$  is the elastic modulus of a regular honeycomb with the same density [17],  $E^m$  is the material elastic modulus, and  $f(\gamma_1) = \sqrt{3}/(0.75 - 1.7625\gamma_1 + 0.9\gamma_1^2 + 0.3625\gamma_1^3)$ . The element thickness ratio  $t_1/t_0$  can be eliminated using Eq. (2), giving the effective elastic modulus at fixed relative density as

$$\frac{E_1}{E_0} = \frac{\sqrt{3}}{4(1 + \gamma_1)^3} f(\gamma_1). \quad (4)$$

For higher order hierarchies, a finite element analysis was implemented using MATLAB. This allowed us to systematically change the geometry of the hierarchical structure and, in particular, to find the geometry, i.e., the set of  $\{\gamma_i\}$ , that maximizes the effective elastic modulus of the honeycomb at a given order of the hierarchy. Figure 2 shows the maximum effective elastic modulus, normalized by the elastic modulus of a regular honeycomb with the same density  $E_0 = 1.5\bar{\rho}^3 E^m$ , for different relative structural densities (i.e., different values of  $\bar{\rho}$ ) as the order of the hierarchy changes. As can be seen from this figure, the maximum effective elastic modulus saturates above a certain number of hierarchical orders. (We note that since the lower order hierarchies are special case of higher orders, the curves in Fig. 2 never reach a local maximum but merely saturate.) For example, for  $0.018 \lesssim \bar{\rho} \lesssim 0.026$ , the maximum modulus is achieved for hierarchical orders  $\geq 6$ . This feature is confirmed by experiments in which unit cells of hierarchical honeycombs with one to four hierarchies were fabricated using 3D printing, maintaining a constant relative density of 0.054 [see Fig. 1(a)]. The fabrication and mechanical testing are described in the Supplemental Material [25]. The experimentally measured effective modulus shows good agreement with that predicted by the numerical simulations, see the inset of Fig. 2.

Figure 2 also shows the behavior of hierarchical structures in which the shear and stretching energies are eliminated from the analysis (dashed curve), so that only the bending energy remains. As the number of hierarchies increases, the

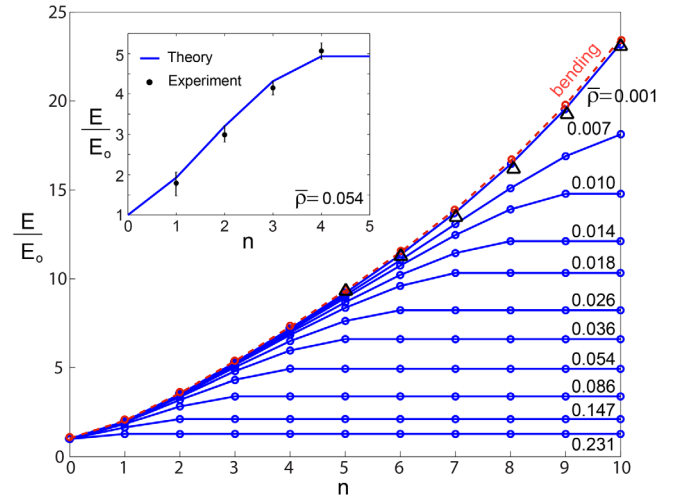


FIG. 2 (color online). Maximum achievable elastic modulus (elastic modulus limit) of hierarchical honeycombs for different relative densities  $\bar{\rho}$  and different hierarchical orders  $n$ , normalized by the elastic modulus of a regular honeycomb of the same density. The numerically computed elastic modulus of hierarchical honeycombs with bending only is shown by the dashed curve. The elastic modulus limit found from our scaling analysis [Eq. (5)] is shown by (triangle) points. The inset shows comparison with the experimental results for hierarchical honeycombs with a density of  $\bar{\rho} = 0.054$ .

effective elastic modulus of this “bending-only” structure increases without bound (as expected since the curvature increases without bound and hence so does the bending energy). We therefore see that at high orders of hierarchy, shear and stretching “soften” the structure: a balance that is crucial in determining the optimal structure. Figure 3 shows how the optimal structural organization, i.e., the set  $\{\gamma_i\}$ , evolves as the relative density changes. As can be seen from this figure, as  $\bar{\rho} \rightarrow 0$ , the values of  $\gamma_i \rightarrow 1/2$  and  $n$  increases.

We now seek to understand these numerical results using a scaling analysis: we seek the maximum amplification of the effective elastic modulus, when replacing a Y-shaped structure by a hexagon. Based on Fig. 3, we assume that  $\gamma_i = 1/2$  in the limit  $\bar{\rho} \ll 1$ , which also ensures that the resulting structure is self-similar. Substituting  $\gamma_1 = 1/2$  into Eq. (3) shows that the effective elastic modulus of the first order bending-only structure [right of Fig. 1(b)] is 1.598 times that of the regular honeycomb [left of Fig. 1(b)]. However, for the first hierarchical order, only three of the

four triangles [shown in pink, Fig. 1(b)] bear the applied load; hence, in calculating the elastic modulus of the composite structure, we must average over the entire area of the composite triangle. Consequently, the amplification of the elastic modulus from one generation to the next is  $3/4 \times 1.598 \approx 1.2$ . Iterating this calculation (and making use of perfect self-similarity) we expect the elastic modulus in bending, normalized by the regular honeycomb, to be  $1.2^n$  where  $n$  is the hierarchical order. Figure 3 suggests that the assumption of perfect self-similarity with  $\gamma = 1/2$  holds only for  $n \geq 5$ ; we take the numerically determined value for the elastic modulus with  $n = 5$  and propose that for  $n \geq 5$  the bending modulus  $E_b$  satisfies

$$\frac{E^b}{E_0} = 9.2 \times 1.2^{n-5}. \quad (5)$$

Equation (5) gives an upper bound for  $n > 5$  and agrees well with the limiting elastic modulus found from finite element simulations as shown in Fig. 2. Using the elastic modulus of a regular honeycomb  $E_0/E^m = 1.5\bar{\rho}^3$  [17], Eq. (5) can be written in terms of the bulk modulus  $E^m$  as

$$\frac{E^b}{E^m} = 5.58 \times 1.2^n \bar{\rho}^3. \quad (6)$$

Note that Eqs (5) and (6) are valid as long as cell walls undergo only bending, which is relevant to the limit of thin beams, i.e., vanishing density. Therefore, to determine the maximum achievable elastic modulus for each order of hierarchy, we also need to compute the shear-based and stretching-based moduli of the structure. For this purpose, we seek the shear energy and stretching energy stored in the zero and first order hierarchical honeycomb. For zero order, the projection of  $F$  perpendicular to the beam is  $F/2$ . The stored shear energy can be written as  $[1/(8/\sqrt{3})]rF^2/(E^m\bar{\rho})$ , where  $r = 2k_s(1 + \nu)$ ,  $\nu$  is the Poisson’s ratio of bulk material, and  $k_s$  is the shear coefficient (equal to  $6/5$  for rectangular cross sections [26]). Therefore, the corresponding stiffness is  $k_0^{\text{sh}}/E^m = (4\sqrt{3}/r)\bar{\rho}$ . For the first order ( $\gamma_1 = 1/2$ ), all the beams have the length  $l_0/4$ . The reaction forces at the midline are shown as  $N_1$  and  $N_2$  [Fig. 1(b)]. The shear energy is determined as  $(\sqrt{3}/8)[r/(E^m\bar{\rho})](F^2 + N_1^2 + 5N_2^2)$ . As  $N_1 + N_2 = F$ , minimizing the energy with respect to  $N_1$  yields  $N_1 = 5F/6$  and  $N_2 = F/6$ . Consequently, the shear energy is  $(11\sqrt{3}/192)rF^2/(E^m\bar{\rho})$ , while the corresponding stiffness is  $k_1^{\text{sh}}/E^m = [32\sqrt{3}/(11r)]\bar{\rho}$ . The shear modulus is multiplied by the ratio  $k_1^{\text{sh}}/k_0^{\text{sh}} = 8/11$ . As we saw in the bending-only case, only  $3/4$  of the structure has its modulus changed. So the shear-based modulus is multiplied by  $(3/4)(8/11) = 6/11 \approx 0.545$ . The shear-based modulus therefore takes the form

$$\frac{E^{\text{sh}}}{E^m} = \frac{2\sqrt{3}}{k_s(1 + \nu)} 0.545^n \bar{\rho}, \quad (7)$$

where  $k_s = 6/5$  for a rectangular cross section [26].

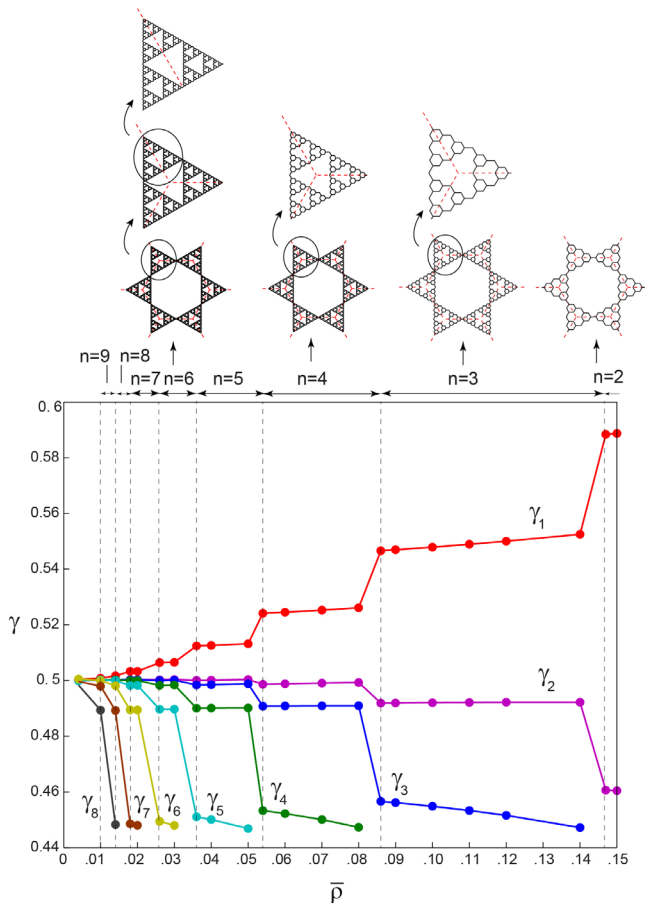


FIG. 3 (color online). Topology of the stiffest hierarchical honeycombs at different relative densities. The results show the values of  $\gamma$  corresponding to the optimum structure of the hierarchical honeycombs at different relative densities. Maximum achievable hierarchical order and selected topologies of the stiffest hierarchical honeycombs in the specified relative density range are also shown at the top.

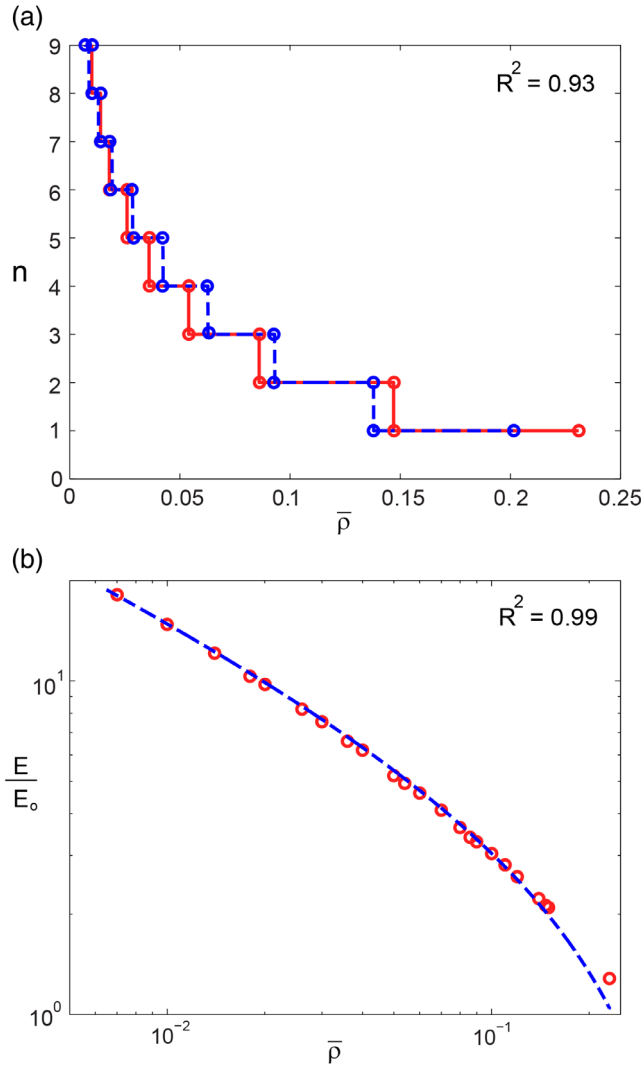


FIG. 4 (color online). (a) The order of hierarchy that yields the stiffest hierarchical honeycomb as a function of the relative density. The results of numerical analysis (solid line) are shown together with scaling analysis results [Eq. (8)] (dashed line). (b) The limiting elastic modulus of the hierarchical honeycomb versus the relative density. The results of numerical analysis (circle markers) are shown together with scaling analysis results [Eq. (9)] (dashed curve).

The above scaling relations show that if the order of hierarchy increases, the bending-based modulus increases while the shear-based modulus decreases. We expect that the elastic modulus of the combined structure should be optimal when  $E^{\text{sh}} \sim E^b$ , yielding

$$n = \lfloor -2.54 \ln \bar{\rho} + c \rfloor, \quad (8)$$

where  $\lfloor \cdot \rfloor$  is the floor function (since  $n$  is an integer). The constant  $c$  can be found from numerical data as  $-3.03$ . Figure 4(a) shows the optimum hierarchical order for different structure densities  $\bar{\rho}$  and shows that the results of our scaling analysis are in good agreement

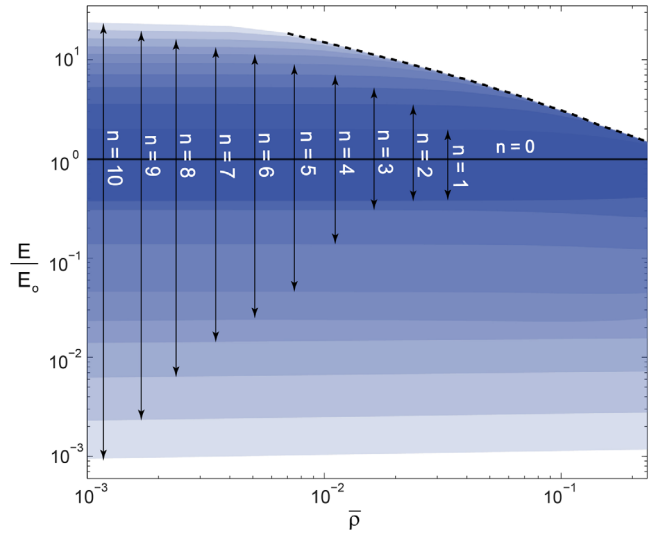


FIG. 5 (color online). Elastic modulus range for different order of hierarchy  $n$  versus relative density. Dashed curve shows the limiting elastic modulus of the hierarchical honeycomb for specified relative density [Eq. (9)].

with the results of finite element simulations especially for small densities ( $R^2 = 0.93$ ). Replacing the value of  $n$  from Eq. (8) in the elastic modulus of Eq. (6) gives the maximum reachable elastic modulus at each density as

$$E/E_0 = c_1 \bar{\rho}^{-0.46} + c_2, \quad (9)$$

where  $c_1 \approx 2.15$  and  $c_2 \approx -3.19$  can be found from numerical data. Figure 4(b) shows the maximum achievable elastic modulus as a function of relative density. The results of scaling analysis are in good agreement with finite element simulations, especially for small densities ( $R^2 = 0.99$ ). (In this analysis, we have neglected the contribution of stretching energy in comparison with the shear energy since the effective spring constant of shear is softer than that for stretching in the limit of large  $n$ .)

Although our focus has been on optimizing the modulus of the structure, our results also show that the effective modulus can be tuned by varying  $\bar{\rho}$  and  $n$ . Figure 5 shows these achievable elastic moduli for  $n \leq 10$ ; the upper bound of this range (dashed curve) shows the maximum achievable elastic modulus for different densities, and is equivalent to that shown in Fig. 4(b). As can be seen from this figure, increasing the hierarchical order while preserving the structural density can significantly increase the effective elastic modulus of the hierarchical structure. Similarly, the maximum achievable hierarchical level is increased by reducing the structural density.

In summary, a new class of fractal-appearing cellular metamaterials is introduced. Our results show that the effective elastic modulus of the developed cellular material can be increased significantly by increasing the hierarchical

order while preserving the structural density. The optimal hierarchical level is also shown to be increased by reducing the structural density. This particular case of hierarchical refinement can be seen as a promising realization of enhancing performance by adding structural hierarchy. Moreover, the current work provides insight into how incorporating hierarchy into the structural organization can play a substantial role in improving the properties and performance of materials and structural systems and introduces new avenues for development of novel meta-materials with tailorable properties.

This work has been supported by the Qatar National Research Foundation (QNRF) under Grant No. NPRP 09-145-2-061. We also thank the support from NSF CMMI Grant No. 1149750.

---

\*vaziri@coe.neu.edu

- [1] A. Ajdari, B. H. Jahromi, J. Papadopoulos, H. Nayeb-Hashemi, and A. Vaziri, *Int. J. Solids Struct.* **49**, 1413 (2012).
- [2] R. Lakes, *Nature (London)* **361**, 511 (1993).
- [3] D. Rayneau-Kirkhope, Y. Mao, and R. Farr, *Phys. Rev. Lett.* **109**, 204301 (2012).
- [4] N. M. Pugno, *Nanotechnology* **17**, 5480 (2006).
- [5] F. Barthelat and H. Espinosa, *Exp. Mech.* **47**, 311 (2007).
- [6] Z. Zhang, Y.-W. Zhang, and H. Gao, *Proc. R. Soc. B* **278**, 519 (2011).
- [7] R. Lakes, *J. Compos. Mater.* **36**, 287 (2002).
- [8] F. Song, J. Zhou, X. Xu, Y. Xu, and Y. Bai, *Phys. Rev. Lett.* **100**, 245502 (2008).
- [9] Y. Sun and N. Pugno, *Materials* **6**, 699 (2013).
- [10] E. Baer, A. Hiltner, and H. Keith, *Science* **235**, 1015 (1987).
- [11] F. Côté, B. P. Russell, V. S. Deshpande, N. A. Fleck, *J. Appl. Mech.* **76**, 061004 (2009).
- [12] S. Kazemahvazi and D. Zenkert, *Compos. Sci. Technol.* **69**, 913 (2009).
- [13] S. Kazemahvazi, D. Tanner, and D. Zenkert, *Compos. Sci. Technol.* **69**, 920 (2009).
- [14] G. W. Kooistra, V. Deshpande, and H. N. Wadley, *J. Appl. Mech.* **74**, 259 (2007).
- [15] H. Fan, F. Jin, and D. Fang, *Compos. Sci. Technol.* **68**, 3380 (2008).
- [16] Z. Tang, N. A. Kotov, S. Magonov, and B. Ozturk, *Nat. Mater.* **2**, 413 (2003).
- [17] L. J. Gibson and M. F. Ashby, *Cellular Solids: Structure and Properties* (Cambridge University Press, Cambridge, England, 1999).
- [18] D. Rayneau-Kirkhope, Y. Mao, and R. Farr, *Phys. Rev. Lett.* **109**, 204301 (2012).
- [19] D. Weaire and J. Kermode, *Philos. Mag. B* **47**, L29 (1983).
- [20] D. Weaire and N. Rivier, *Contemp. Phys.* **25**, 59 (1984).
- [21] T. Herdtle and H. Aref, *Philos. Mag. Lett.* **64**, 335 (1991).
- [22] B. Haghpanah, R. Oftadeh, J. Papadopoulos, and A. Vaziri, *Proc. R. Soc. A* **469**, 0022 (2013).
- [23] R. Oftadeh, B. Haghpanah, J. Papadopoulos, A. Hamouda, H. Nayeb-Hashemi, and A. Vaziri, *Int. J. Mech. Sci.* **81**, 126 (2014).
- [24] R. Christensen, *J. Appl. Mech.* **54**, 772 (1987).
- [25] See Supplemental Material at <http://link.aps.org/supplemental/10.1103/PhysRevLett.113.104301> for details on the experimental setup and analytical modeling.
- [26] A. Boresi and R. Schmidt, *Advanced Mechanics of Materials* (John Wiley & Sons, New York, 2003).